NeuroImage: Clinical 21 (2019) 101668

Contents lists available at ScienceDirect

NeuroImage: Clinical

journal homepage: www.elsevier.com/locate/ynicl

Gender-specific structural abnormalities in major depressive disorder revealed by fixel-based analysis

Matt Lyon[a], Thomas Welton[a], Adrina Varda[a,b], Jerome J. Maller[a,c], Kathryn Broadhouse[a], Mayuresh S. Korgaonkar[d], Stephen H. Koslow[e], Leanne M. Williams[d,f], Evian Gordon[a,g], A. John Rush[h,i,j], Stuart M. Grieve[a,k,*]

[a] Sydney Translational Imaging Laboratory, Heart Research Institute & Charles Perkins Centre, Sydney Medical School, University of Sydney, NSW 2006, Australia
[b] School of Medicine, University of Notre Dame, Sydney, Australia
[c] General Electric Healthcare, Richmond, Victoria, Australia
[d] The Brain Dynamics Centre, Westmead Millennium Institute and Sydney Medical School, Sydney, NSW, Australia
[e] Department of Psychiatry and Behavioral Sciences, University of Miami Miller School of Medicine, Miami, FL 33136, USA
[f] Sierra-Pacific Mental Illness Research, Education, and Clinical Center (MIRECC) Veterans Affairs Palo Alto Health Care System, Palo Alto, CA 94304, USA
[g] Brain Resource Ltd, San Francisco, CA, USA
[h] Duke-National University of Singapore, Singapore
[i] Department of Psychiatry, Duke Medical School, Durham, NC, USA
[j] Texas Tech University-Health Sciences Center, Permian Basin, TX, USA
[k] Department of Radiology, Royal Prince Alfred Hospital, Camperdown, Sydney, NSW 2006, Australia

ARTICLE INFO

Keywords:
Magnetic resonance imaging
Diffusion tensor imaging
Major depressive disorder
Biomarker predictors
Remission
iSPOT-D

ABSTRACT

Background: Major depressive disorder (MDD) is a chronic disease with a large global impact. There are currently no clinically useful predictors of treatment outcome, and the development of biomarkers to inform clinical treatment decisions is highly desirable.

Methods: In this exploratory study we performed fixel-based analysis of diffusion MRI data from the International Study to Predict Optimized Treatment in Depression with the aim of identifying novel biomarkers at baseline that may relate to diagnosis and outcome to treatment with antidepressant medications. Analyses used MR data from individuals with MDD (n = 221) and healthy controls (n = 67).

Results: We show focal, gender-specific differences in the anterior limb of the internal capsule (males) and bilaterally in the genu of the corpus callosum (females) associated with diagnosis. Lower fibre cross-section in the tapetum, the conduit between the right and left hippocampi, were also associated with a decreased probability of remission. Analysis of conventional fractional anisotropy showed scattered abnormalities in the corona radiata, cerebral peduncles and mid-brain which were much lower in total volume compared to fixel-based analysis.

Conclusions: Fixel-based analysis appeared to identify different underlying abnormalities than conventional tensor-based metrics, with almost no overlap between significant regions. We show that MDD is associated with gender specific abnormalities in the genu of the corpus callosum (females) and in the anterior limb of the internal capsule (males), as well as gender-independent differences in the tapetum that predict remission. Diffusion MRI may play a key role in future guidance of clinical decision-making for MDD.

1. Introduction

Major depressive disorder (MDD) is the leading cause of disability for individuals in early and middle adulthood, and affects approximately 216 million people annually (Vos et al., 2016). The rate of remission with front-line anti-depressant medications (ADMs) is just 34% (Trivedi et al., 2006), hence there is a need for translatable biomarkers to improve clinical decision making in MDD. Recent advances in structural magnetic resonance imaging (MRI) analysis techniques have enabled large improvements in sensitivity (Callaghan et al., 2018).

* Corresponding author at: Sydney Translational Imaging Laboratory, Heart Research Institute, Sydney Medical School & Charles Perkins Centre, University of Sydney, Camperdown, NSW 2006, Australia.
E-mail address: stuart.grieve@sydney.edu.au (S.M. Grieve).

https://doi.org/10.1016/j.nicl.2019.101668
Received 14 July 2018; Received in revised form 23 November 2018; Accepted 4 January 2019
Available online 08 January 2019

It is therefore pertinent to investigate the potential for MRI-based markers of structural brain abnormalities in MDD using state-of-the-art tools. In this paper we evaluate fixel-based analysis (FBA) (Raffelt et al., 2017), a new technique for the analysis of diffusion imaging (dMRI), using data from the international Study to Predict Optimized Treatment in Depression (iSPOT-D).

It is now well established that MDD is associated with structural brain abnormalities. A large meta-analysis found that hippocampal volume normalized in remitted patients (Kempton et al., 2011), and our group recently demonstrated that hippocampal tail volume is predictive for both diagnostic status and remission (Maller et al., 2017). In white matter (WM) numerous abnormalities in MDD have been identified previously; for example, we proposed a metric derived from diffusion measurements in the fornix and the cingulate bundle which had significant discriminatory power to predict non-remission (Korgaonkar et al., 2014). These abnormalities are primarily localised to the limbic network, which is central to emotion and memory, and to the frontal association fibres, which interconnect the cortex of the frontal lobe (Drevets et al., 2008; Rigucci et al., 2010). Data from iSPOT-D have also revealed widespread regions of gray matter atrophy, providing converging evidence of the structural contribution to the development of MDD (Grieve et al., 2013b). Gender specific structural differences have also been found in other mental disorders such as bipolar (Bora et al., 2012; McLean et al., 2011); however WM gender analysis has not yet been studied within MDD. These and other data from the literature highlight the potential for dMRI as a biomarker in MDD (Chi et al., 2015).

The key type of analysis applied in many of these studies has utilised a diffusion-tensor model of dMRI data. Diffusion-tensor imaging (DTI) uses a Gaussian model of diffusion to fit a single tensor at each voxel. However, given that as much as 90% of the brain's WM comprises two or more fibre populations (Jeurissen et al., 2013), a single tensor is not sufficient to accurately model crossing fibres. As such, any metrics derived from a tensor model, including fractional anisotropy (FA), are impacted by this issue. New techniques have been developed specifically to model crossing fibres. One such technique utilizes constrained spherical deconvolution (CSD) to produce a fibre orientation distribution (FOD); a continuous distribution that represents the partial volume of underlying fibres as a function of orientation (Tournier et al., 2004).

FBA is a new type of dMRI analysis based on the FOD that may reveal different microstructural changes within the brain (Raffelt et al., 2017). A fixel, which refers to the fibre population within a voxel, is determined via segmentation of the FOD lobes (Raffelt et al., 2015). Probabilistic tracking then defines connectivity between fixels, which is used for connectivity-based smoothing and connectivity-based fixel enhancement to increase statistical power. FBA produces three metrics: fibre density (FD), fibre cross-section (FC), and fibre density cross-section (FDC), summarized in Fig. 1. FD refers to the apparent fibre density that is derived from the FOD (Raffelt et al., 2012). FC is an estimation of the fibre bundle area perpendicular to the length of the fibre. Since microstructural damage may impact either FD or FC independently, the FDC (as the product of the two) acts as a summary measure. Using this method, different and a greater volume of WM abnormalities may be detected than compared with conventional diffusion-tensor based metrics; this has so far only been applied in motor-neurone disease (Raffelt et al., 2015), Alzheimer's disease (Mito et al., 2017) and in a mouse model of traumatic brain injury (Wright et al., 2017). In this exploratory study we hypothesised (a) that FBA would reveal abnormal WM microstructure in MDD, which would be localised to the limbic network and frontal association fibres as well as being associated with demographic factors including gender and remission. And (b) that FBA would detect different abnormalities compared to conventional metrics derived from the diffusion tensor.

2. Methods and materials

2.1. Participant characteristics and study protocol

The Western Sydney Ethics Committee approved this study, and all participants provided written informed consent. Data were gathered from participants in the iSPOT-D trial, which has been described previously (Grieve et al., 2013a; Williams et al., 2011). The Mini-International Neuropsychiatric Interview (Sheehan et al., 1998) using DSM-IV criteria (American Psychiatric Association, 2000) and a 17-item Hamilton Rating Scale for Depression ($HDRS_{17}$) (Hamilton, 1960) score ≥ 16 confirmed the primary diagnosis of MDD. Exclusion criteria of the iSPOT-D trial ensured that no participant had suicidal ideations and/or tendencies, bipolar disorder, psychosis, any primary eating disorder, post traumatic stress disorder, obsessive compulsive disorder, post-natal depression or any axis II personality disorder, as diagnosed using the Mini-International Neuropsychiatric Interview (Sheehan et al., 1998) or by a health care professional. All MDD participants were either ADM-naïve or had undergone a wash-out period of at least 5 half-lives of a previously prescribed ADM.

Participants were randomized to receive flexibly-dosed, open-label escitalopram, sertraline or venlafaxine-extended release for eight weeks. The study recruited from primary care, community and academic psychiatry settings with the goal of representing a broad sample of antidepressant treatment seekers. Medications were prescribed, and doses adjusted by treating clinicians according to routine clinical practice, following the recommended dose ranges. A $HDRS_{17}$ of ≤7 after 8 weeks was used to define remission (Maust et al., 2012). Duration of depression was also recorded.

Data were drawn from the imaging arm of the iSPOT-D study, consisting of 232 subjects diagnosed with MDD and 68 controls. Demographic and clinical data were obtained at baseline, including age, gender, age at first MDD diagnosis, and depression duration. Baseline MRI sequences were obtained on all participants, as described below. DWI data were visually inspected and of the total 300 dMRI datasets; 12 (11 MDD, 1 control) were unusable due to motion artefact,

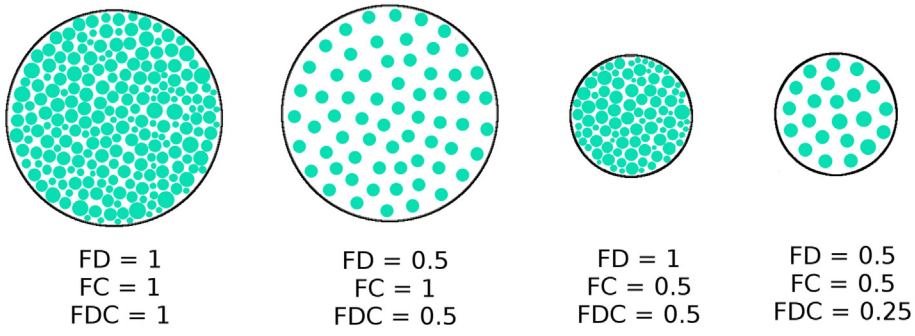

Fig. 1. Schematic showing cross sections of fibre bundles with varying fibre density, fibre cross-section, and fibre density. Each green dot represents the cross section of a single axon. FDC is the product of FD and FC, and is therefore sensitive to changes in both metrics (Figure adapted from Raffelt et al. (Raffelt et al., 2017)).

leaving 221 MDD and 67 control datasets usable for analysis. Of the remaining 221 MDD participants, 43 did not complete an 8-week follow-up assessment and were therefore excluded from additional treatment analysis.

2.2. Image acquisition

MRI data were acquired using a 3 Tesla GE Signa HDx scanner (GE Healthcare, Milwaukee, Wisconsin), using an 8-channel head coil. Diffusion images were acquired using a spin-echo EPI sequence. Seventy contiguous 2.5 mm slices were acquired in an axial orientation with an in-plane resolution of 1.72 mm × 1.72 mm and a 128 × 128 matrix (TR: 17000 ms; TE: 95 ms; Fat Saturation: ON; NEX: 1; Frequency direction: R/L). Four b = 0 volumes and 42 unique diffusion-weighted volumes were acquired with a b-value of 1250 s/mm^2. T1-weighted images were acquired using a contiguous AC-PC aligned sagittal IR-SPGR sequence (TR = 8.3 ms, TE = 3.2 ms, TI = 500 ms, flip angle = 11 degrees, matrix = 256 × 256, voxel dimensions = 1 mm isotropic, NEX = 1).

2.3. Fixel-based analysis

FBA was performed using the MRtrix3 package (Brain Research Institute, Melbourne, Australia; http://mrtrix.readthedocs.io/en/latest/). This software utilizes the principles of CSD and probabilistic streamlines to define the anatomical circuitry of the brain, especially that of the WM structure. Diffusion data were denoised (Veraart et al., 2016), and pre-processed for eddy current and motion correction using FSL (Andersson et al., 2003; Andersson and Sotiropoulos, 2016) as per the recommended pipeline (Raffelt et al., 2012). The data were then corrected for spatial intensity inhomogeneity using N4 bias correction (Tustison et al., 2010), and normalized to the median b = 0 WM signal. The data were then up-sampled to 1.25 mm voxel size to improve downstream spatial normalization statistics (Dyrby et al., 2014). FODs were calculated using MRtrix3 by means of a group averaged response function. A study-specific FOD template comprising 40 gender and group-matched datasets was generated, to which all subjects and subsequent image data were registered to. The template was then used to generate a WM fixel template that was used to identify the best fixel correspondence across subjects. Values for FD, FC, and FDC were then calculated. The natural logarithm of FC was calculated and used for downstream statistics, to ensure the data were centred about zero and normally distributed. Whole brain fibre tractography was performed on the FOD template (number of streamlines = 20 million, maximum angle = 22.5, maximum fibre length = 250 mm, minimum fibre length = 10 mm). SIFT (Spherical-deconvolution Informed Filtering of Tractograms (Smith et al., 2013)) was then performed to reduce tractography biases, which reduced the number of tracks to 2 million.

Non-parametric permutation testing was performed using connectivity-based fixel enhancement (Raffelt et al., 2015) via the MRtrix3 package. In summary, this approach uses information from probabilistic tractography to identify fixels that are likely to belong to the same anatomical structures or pathology and applies smoothing in a tract-specific manner. Then, a threshold-free cluster enhancement-like approach is used to identify clusters of interest. 5000 random permutations of the sample were used to determine statistical significance.

2.4. Diffusion tensor imaging analysis

As a comparison to the conventional method, DTI based voxel-wise analysis was performed using the FSL diffusion toolkit (FDT; version 5.0.9). dMRI data were denoised then corrected for eddy currents and motion. DTI metrics were then generated for FA, Apparent Diffusion Coefficient (ADC), Axial Diffusivity (AD), and Radial Diffusivity (RD). DTI metrics were then co-registered to MNI space using FSL FNIRT via T1-weighted data. Typically, tract-based spatial statistics (TBSS) is used to perform voxel-wise analysis of DTI derived metrics (Smith et al., 2006) on a tract skeleton calculated from voxels with high FA. As FBA metrics are calculated using the whole brain, DTI metrics were also calculated using whole-brain voxel-wise analysis instead of TBSS. To allow a direct comparison between DTI and FBA metrics, the study-specific WM template, as described previously, was used as a mask for DTI analysis. Voxel-wise cross-subject statistical analysis was performed using randomise (Winkler et al., 2014) with threshold-free cluster enhancement and 5000 permutations (Smith and Nichols, 2009). Each nonparametric permutation test for FA, ADC, AD, and RD analysis resulted in an image where the voxel value represented the FWE-corrected *p*-value, visualised as (1-p). An FWE-corrected p-value < .05 was considered statistically significant. Anatomical regions were identified using the ICBM-DTI-81 white-matter atlas (Mori and Crain, 2006) and the JHU white-matter tractography atlas (Hua et al., 2008).

2.5. Statistical analysis

Age and gender were demeaned and included as covariates in all models where applicable. An exploratory univariate analysis at the group level determined the factors to be included in each model, with variables being marked as "significant" ($p < 0.05$) or "borderline significant" ($0.05 < p < 0.10$; Table 1). $HDRS_{17}$ was not considered as a potential covariate because it was used to define remission. All comparisons were tested for in both fixel-based data and diffusion tensor data. The first comparison was between MDD and control groups, with age and gender (both demeaned) as covariates. The cohort was then split into male and female subgroups, where MDD vs controls were tested for in the respective subgroup. Age was again demeaned (mean was calculated for the cohort in question, e.g. males only) and included as a covariate in these models. Next, remission was compared against non-remission within the MDD cohort. This model included age, gender, and years of education as co-variates. Years of education was borderline significant in the univariate analysis and therefore included ($0.05 < p < 0.10$). Lastly, the MDD cohort was subdivided into male and female subgroups, where remission vs non-remission was tested for. Age was demeaned and included as a covariate.

Table 1
Demographics and clinical measures summary.

Characteristics	Controls		MDD		Remitters		Non-Remitters	
Number (%)	67 (23)		221 (77)		59 (33)		119 (67)	
% Females	51		52		53		50	
	Mean	SD	Mean	SD	Mean	SD	Mean	SD
Age (years)[a]	30.3	12.8	33.6	11.7	30.1	8.7	35.0	12.2
Years of Education[b]	14.7	2.6	14.2	2.7	15.0	2.5	14.2	2.7
Age of Onset (years)	N/A	N/A	21.8	10.3	20.2	8.3	22.2	10.3
MDD Duration (years)	N/A	N/A	11.8	10.6	10.0	8.6	12.9	11.1
Number of MDD Episodes	N/A	N/A	11.8	18.9	9.4	15.4	12.2	19.2
$HDRS_{17}$ Baseline	N/A	N/A	21.4	3.7	21.3	3.7	21.5	3.7
$HDRS_{17}$% change[c]	N/A	N/A	N/A	N/A	−77.6	8.2	−38.1	18.7

[a] MDD vs controls significant $p < 0.05$.
[b] Remission vs non-remission borderline significant $0.05 < p < 0.10$.
[c] Percentage change after 8 weeks, negative number indicates a decrease in $HDRS_{17}$ after 8 weeks; $HDRS_{17}$ = Hamilton Depression Rating Scale, SD = Standard deviation.

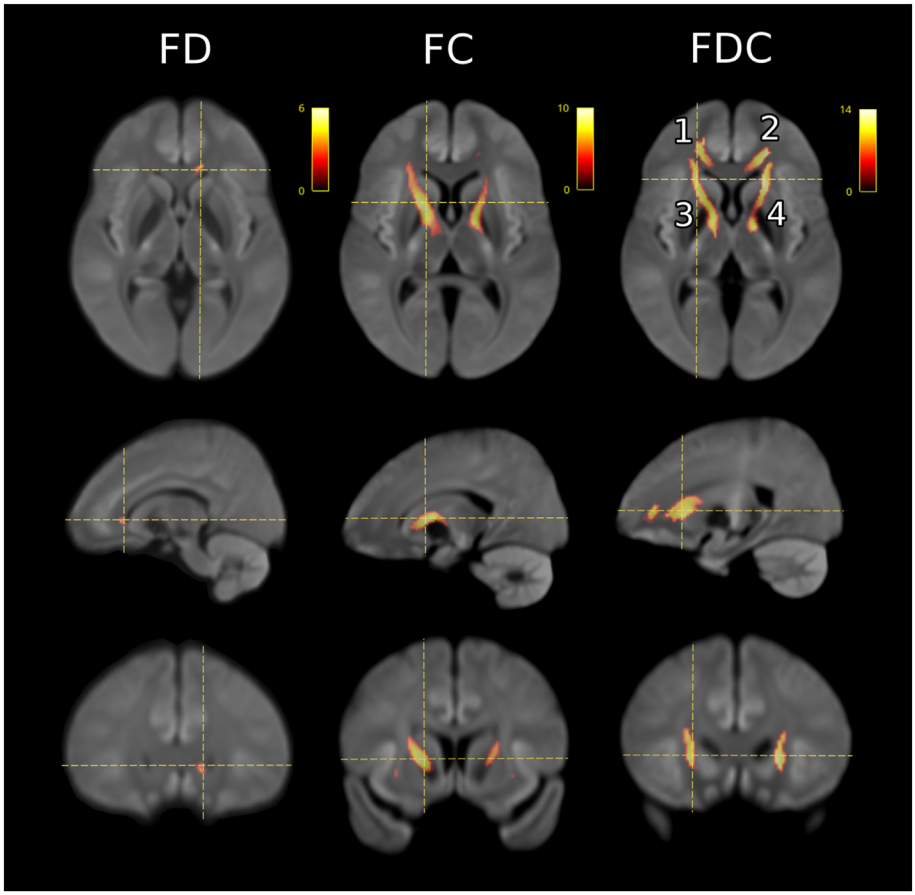

Fig. 2. FBA comparison between MDD (n = 221) and controls (n = 67) for FD, FC, and FDC with age and gender as covariates (demeaned). Images were rendered on a study-generated WM template. The coloured voxels represent significance ($p < 0.05$) in control greater than MDD, whilst the scale represents the percentage difference relative to controls. Cluster (1) is located anatomically in the right frontal projection of the corpus callosum, (2) in the left frontal projection of the corpus callosum, (3) in the right anterior limb of the internal capsule, and (4) in the left anterior limb of the internal capsule.

3. Results

3.1. Participant characteristics

Table 1 shows the clinical and demographic characteristics of the whole cohort by diagnosis, and for the MDD group subdivided by remission status at 8 weeks. A small difference in age was present between MDD subjects and controls (33.6 years vs 30.3 years; $F(1,286) = 3.967$, $p = 0.047$).

43 MDD participants did not complete an 8-week follow-up, therefore 178 MDD participants contributed to the remission vs. non-remission analysis. Participants who remitted were significantly younger than those who did not (30.1 years vs 35.0 years; $F(1,176) = 7.566$, $p = 0.007$). MDD duration was not significantly different between males and females, nor between those who did and did not remit ($p > 0.05$). Years of education was borderline significant ($0.05 < p < 0.10$) between remitters and non-remitters.

3.2. Whole brain FBA of MDD versus controls

Fig. 2 illustrates the significant regions of altered metrics for the FBA analysis of MDD ($n = 221$) versus controls ($n = 67$). Focal differences in magnitude of −5 to −9% were seen in MDD compared to controls across all three FBA metrics. Table 2 summarizes the location, volume and percentage difference of the significant clusters. The differences were symmetric, and involved two anatomical regions: the genu of the corpus callosum (CC) and bilateral associated frontal projection fibres (Clusters 1 and 2), and the anterior limb of the internal capsule, with extension medially to involve the cerebral peduncles of the midbrain (Clusters 3 and 4).

FC showed an average percentage difference relative to controls of −5.8% and − 6.0% in the left and right anterior limb of the internal capsule, respectively, compared to −7.4% and − 7.8% in the same cluster location for FDC. FD presented a mean percentage difference of −5.0% in the left frontal projection of the genu of the CC, compared to −7.0% for FDC in the same ROI, and − 9.0% in the right frontal projection.

Table 2
Significant clusters of FBA metrics for MDD versus controls.

Cluster	Volume *mL* (voxels)	p-value (min)	T-value (max)	% Difference		MNI co-ordinates		
				(mean)	(max)	x	y	z
FDC, Control > MDD								
2 & 4	3.16 (3161)	0.003	5.72	−8.9	−13.4	−18	21	4
3	2.88 (2875)	0.001	5.73	−8.4	−11.0	19	12	5
1	1.05 (1053)	0.008	4.84	−9.0	−11.9	18	42	−1
FC, Control > MDD								
3	3.92 (3919)	< 0.001	7.03	−6.0	−9.3	18	9	4
4	2.17 (2166)	0.004	5.54	−5.8	−8.0	−15	−2	0
FD, Control > MDD								
2	0.04 (39)	0.024	3.79	−5.0	−5.73	−11	32	−1

1, Right frontal projection of the corpus callosum (CC), 2, Left frontal projection of the CC, 3, Right anterior limb of the internal capsule, 4, Left anterior limb of the internal capsule.

3.3. Differential gender effects

To test the potential impact of gender, FBA analysis was performed

Table 3
Summary of gender differences.

Cluster	Volume *mL* (voxels)	p-value (min)	T-value (max)	% Difference		MNI co-ordinates		
				(mean)	(max)	x	y	z
FDC, Male, Control > MDD								
3	0.88 (880)	0.010	5.53	−11.1	−15.5	19	13	6
FC, Male, Control > MDD								
3	0.68 (680)	0.014	4.89	−6.8	−8.6	17	7	6
FDC, Female, Control > MDD								
1/2	1.47 (1466)	0.008	4.61	−10.1	−14.0	2	37	1
FC, Female, Control > MDD								
5	1.73 (1725)	0.012	3.30	−5.7	−7.9	−1	−41	23
3	0.93 (929)	0.006	5.58	−7.7	−10.1	14	1	1
6	0.1 (100)	0.022	4.27	−5.8	−6.9	39	−33	8
1	0.06 (63)	0.036	3.64	−6.9	−7.7	15	33	9
2	0.06 (62)	0.040	2.80	−5.9	−6.4	−15	36	8

1, Right frontal projection of the corpus callosum (CC), 2, Left frontal projection of the CC, 3, Right anterior limb of the internal capsule.4, Left anterior limb of the internal capsule, 5 Tapetum, 6, Right inferior longitudinal fasciculus.

on a cohort of males only (MDD $n = 106$, control $n = 33$) and then females only (MDD $n = 115$, control = 34). The two tests revealed significant clusters corresponding to those described in the group comparison. These results are summarized in Table 3 and Fig. 3. It was found that, for FDC, females showed significant control > MDD only in the anterior anatomical locations detected in the group comparison; namely, the entire genu of the CC, encompassing Clusters 1 and 2 (Fig. 3a). The average percentage difference of this region was 10% lower compared to controls. No significant clusters were detected corresponding to Clusters 3 and 4 in females. Conversely, in males, only the right anterior limb of the internal capsule was significant in FDC (Cluster 3; Fig. 3a). The average percentage difference in this cluster was −11% compared to controls.

Separate gender-specific analysis of the FC revealed five significant clusters in females incorporating small volumes concordant with

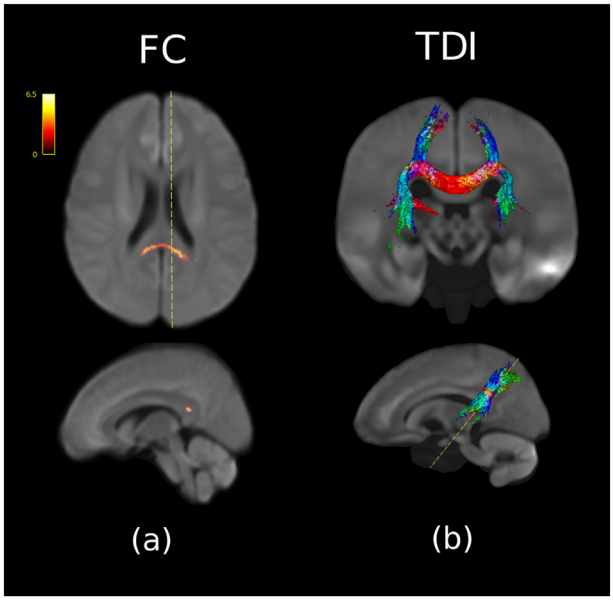

Fig. 4. Comparison between remission (n = 59) and non-remission (n = 119) for FC controlling for age, gender, and years of education. (a) The coloured voxels represent significance ($p < 0.05$) in non-remission greater than remission, whilst the scale represents the percentage difference relative to non-remission. (b) The DEC TDI was created using tractography seeded from the significant ROI.

Clusters 1, 2, and 3, as well as two additional locations not present in the whole group analysis. These clusters showed an average difference in FC ranging from −5 to −8%. The largest cluster not previously detected was located within the tapetum (termed Cluster 5; Fig. 3b). The anatomical connectivity of this cluster was estimated by using unconstrained tractography seeded from the cluster voxels (Fig. 3c). Streamlines seeded in an ROI generated from Cluster 5 can be seen to extend superoinferiorly in a distribution conforming to the known anatomy of the tapetum (Pustina et al., 2014). The second new cluster (Cluster 6) of lower FC in female MDD patients was located in the right inferior longitudinal fasciculus and had a volume of 0.1 mL.

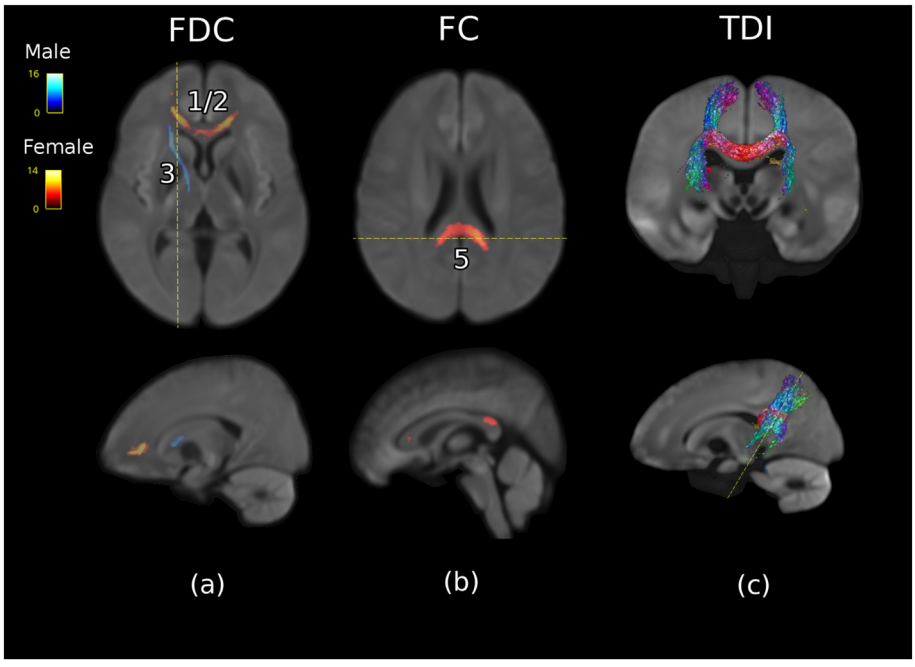

Fig. 3. Comparison of significant voxels in FBA for male (MDD n = 106, control n = 33) and female cohort (MDD n = 115, control $n = 34$). The colour scale represents the percentage difference relative to controls. (a) FDC significant voxels in female (red) cohort and male cohort (blue). (b) FC significant voxels in female cohort (red), male cohort has no significant voxels in this slice. (c) To confirm the anatomical location of Cluster 5, A directionally encoded colour (DEC) tract density image (TDI) was created using tractography seeded from Cluster 5. Cluster (1/2) is located anatomically in the frontal projection of the corpus callosum bilaterally, (3) in the right anterior limb of the internal capsule, and (5) in the tapetum.

A single cluster was detected for lower FC in male MDD patients which corresponded to Cluster 3 from the whole group analysis and was associated with an average difference of −6.8%. No significant gender-specific differences in FD were detected.

3.4. FBA analysis of remission vs non-remission

Fig. 4 summarizes an analysis of FBA metrics for the comparison of remitters (n = 59) vs non-remitters (n = 119), showing a single contiguous cluster of higher FC associated with positive remission status. No other FBA metrics were significant. The significant cluster represented a + 6.5% average difference in FC compared to non-remitters, located in the tapetum. This region showed an overlap with the female-only cluster (Cluster 5) in the control > MDD analysis. The anatomical connectivity of this cluster was also estimated using tractography (Fig. 4b). A post-hoc analysis of remission vs non-remission in the male only (remission n = 27, non-remission n = 59) and female only (remission n = 32, non-remission n = 60) subgroups revealed no significant remission clusters.

3.5. Evaluation of DTI-metrics

To compare the performance and evaluate any differences in patterns of structural difference we replicated all the previously mentioned comparisons using a standard voxel-based analysis approach, focussing on the DTI-based metric, FA. A secondary set of analyses was also performed on previous contrasts using ADC, AD, and RD, as less commonly used but still biologically-meaningful measurements.

Fig. 5a and Table 4 summarise the significant regions of lower FA seen in the MDD cohort compared to controls. For the control > MDD analysis, FA demonstrated significant clusters in four regions: the left anterior corona radiata, the left external capsule, the cerebral peduncle bilaterally, and in the anterior aspect of the mid-brain. There was minimal overlap between these smaller clusters and the FDC clusters (total volume of overlap = 0.27 mL; Fig. 5).

Our secondary analysis showed a widespread number of small diffuse clusters of lower AD in MDD compared to controls (all 1.2 mL or less in volume). These are shown in Fig. 5b and were located in the splenium of the CC, the left posterior corona radiata, the superior longitudinal fasciculus bilaterally, and the left posterior thalamic radiation. ADC showed one small cluster in the left anterior thalamic radiation, whilst RD had no significant clusters for this contrast.

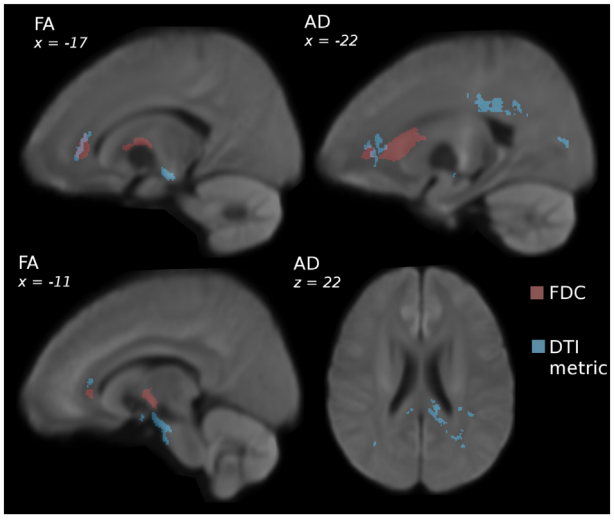

Fig. 5. Comparison between DTI and FBA metrics in MDD (n = 221) vs controls (n = 67). Images were rendered on a study-generated WM template registered to MNI space. The coloured voxels represent significance (1-p where p < 0.05) for the contrast controls > MDD with age and age and gender as covariates (demeaned).

Table 4
Significant clusters in the analysis of DTI-based metrics.

Volume mL (voxel)	p-value (min)	T-value (max)	% Difference (mean)	MNI co-ordinates		
				x	y	z
FA, Control > MDD						
1.36 (1361)	< 0.001	6.85	−13.9	−9	−16	−18
0.93 (929)	0.001	5.58	−13.5	13	−14	−18
0.66 (657)	0.009	4.59	−8.5	−18	38	6
0.58(575)	0.006	5.51	−11.0	−28	15	−7
0.07 (70)	0.017	5.78	−18.6	−8	2	−16
0.06 (62)	0.020	5.52	−20.0	7	4	−17
AD, Control > MDD						
1.18 (1182)	0.016	4.77	−4.3	−30	−48	28
0.99 (986)	0.019	4.85	−5.1	−10	−40	21
0.88 (879)	0.022	4.29	−4.1	−21	−33	33
0.79 (785)	0.021	4.38	−6.9	−20	38	4
0.25 (252)	0.030	4.19	−5.7	−30	−58	15
0.24 (239)	0.023	4.86	−7.3	46	−42	1
0.17 (173)	0.022	4.72	−7.1	−24	−82	7
0.10 (101)	0.042	3.52	−4.5	−27	−20	39
0.09 (85)	0.039	4.27	−5.8	11	−42	16
ADC, Control > MDD						
0.07 (73)	0.035	5.07	−5.2	−23	−52	38
FA, MDD > Control						
0.32 (316)	0.020	4.55	6.6	25	−26	27
0.31 (305)	0.007	5.22	7.9	23	−22	9
ADC, MDD > Control						
0.07 (74)	0.025	6.77	21.4	−1	−19	−15
RD, MDD > Control						
0.20 (208)	0.005	6.78	23.0	0	−19	−16
0.19 (186)	0.019	5.41	38.6	−9	−13	−18

FA, ADC, and RD all showed small scattered significant clusters for the MDD > control contrast, whilst AD did not reveal any significant voxels. For FA, there were significant clusters in the right posterior limb of the internal capsule, and in the right superior corona radiata. ADC and RD had small significant clusters (see Table 4). No significant clusters were detected for the DTI-metrics for the contrast of remission vs non-remission.

A gender split analysis of DTI metrics revealed significant clusters only in the female cohort. Only FA and AD in control > MDD reached significance. FA had many diffuse clusters that were located in the genu of the CC (Clusters 1 and 2), the cerebral peduncle bilaterally, and the left uncinate fasciculus. AD had one significant cluster in Cluster 2. These results are summarized in Table 5.

No significant clusters were detected for the remission vs non-

Table 5
Significant clusters in the analysis of gender effects for DTI-based metrics.

Volume mL (voxel)	p-value (min)	T-value (max)	% Difference (mean)	MNI co-ordinates		
				x	y	z
FA, Female, Control > MDD						
1.07 (1065)	0.001	6.70	−18.1	−10	−14	−18
0.92 (923)	0.003	5.52	−10.2	−14	35	7
0.84 (835)	0.002	5.13	−18.4	11	−13	−18
0.49 (488)	0.008	5.09	−16.0	−30	12	−10
0.26 (260)	0.009	5.33	−19.4	2	7	−5
0.24 (239)	0.002	6.29	−17.3	0	−19	−15
0.19 (188)	0.007	5.58	−21.2	25	−1	−12
0.12 (122)	0.005	6.33	−26.8	−22	−1	−11
0.11 (110)	0.016	5.01	−24.6	9	2	−16
0.09 (90)	0.010	5.94	−26.4	−9	1	−16
0.07 (68)	0.018	4.83	−18.4	−2	4	5
AD, Female, Control > MDD						
0.17 (171)	0.025	4.59	−16.0	−14	30	4

remission gender split analysis of DTI metrics.

4. Discussion

Our data demonstrate strong evidence of WM abnormalities within the brain of MDD patients using FBA. The predominant differences between MDD patients and controls involved areas of lower fibre density cross-section with magnitude of 10% or more across three specific sites: (1) the genu of the corpus callosum, (2) the bilateral frontal projections and (3) the anterior limb of the internal capsule. We also found that these differences were gender-specific. FBA revealed structural features at baseline that were related to remission status, again involving the tapetum – an area not previously highlighted using structural MRI as being associated with remission. FBA played a critical role in enabling the above findings, as examining the same cohort did not detect any substantial difference in the same regions using the conventional DTI-based metric, FA.

Our results have a three-fold importance: (1) methodologically, (2) from a disease mechanism perspective and (3) as an enabler of precision medicine. First, our results suggest that FBA revealed a higher volume of WM microstructural abnormalities compared to conventional DTI-based metrics such as FA, and provide evidence that these two methods may be sensitive to different WM abnormalities. Second, our results have great mechanistic significance: they add convergent information to prior data, both from our iSPOT-D study and other work, which highlight the primacy of two separate networks in the pathophysiology of MDD - the limbic network, and the frontal association network. In particular, the strong association between FBA measurements within the tapetum at baseline to remission status at 8 weeks supports the argument that these structural differences have a *functional significance,* and are not merely secondary to a more primary process. Third, and most importantly, we show that there is a clear difference between the WM abnormalities present in males and females. Given the poor remission rate to conventional ADM treatment, stratification of patients into biological sub-types is of clear future importance.

The presence of gender-specific findings is consistent with the well-established gender differences in incidence and temporal course of various mental disorders (Boyd et al., 2015; Kuehner, 2017; McLean et al., 2011). Prior structural imaging studies have been underpowered to evaluate for subtle brain differences, or have not included a gender analysis (Chi et al., 2015). The lack of overlap between male and female WM differences in MDD revealed using FBA shows the importance of considering gender in any future attempts to develop imaging-guided precision medicine tools, and to adequately power studies to permit this.

The involvement of the tapetum is a unique finding. This structure represents the direct connection between the hippocampi and, as such, the involvement of this structure in the current study suggests that MDD is not only related to ipsilateral connectivity, but also contralateral temporal connectivity. The notion that this significant region (Cluster 5) formed part of the tapetum was supported by tractography. An abnormality in the tapetum relating to both remission and to diagnosis (in females) provides further convergent evidence of widespread limbic abnormalities in depression.

Our FA and AD findings are in concordance with previous DTI studies (Bergamino et al., 2017; Jiang et al., 2017; Shen et al., 2017), with differences in the left superior longitudinal fasciculus, left posterior thalamic radiation and the left posterior corona radiata. Previous studies have also reported lower FA in anterior frontal CC projections (Yamada et al., 2015). Of note, different regions were detected using FBA compared with diffusion tensor-based metrics, such as FA and ADC. Although FBA clearly had a higher volume of significant regions compared to FA or other DTI-metrics, it is also clear that these different analysis types may be weighted with a bias toward detecting different underlying abnormalities, since there was only minimal anatomical overlap between the two analyses in our study.

Our study has several limitations. Primary among these is the cross-sectional nature of our baseline analysis. Future longitudinal work is required to determine if the structural differences observed are a product of a depression state, preceding causal factors or a combination of both. While our data have been acquired using sufficient angular resolution to provide a valid and robust analysis, the acquisition is not optimal for an FOD based approach. The relatively low acquired b-values limit the interpretation of changes in FD, as such the values likely reflect not just the intra-axonal component, but some of the extra-cellular component as well. In the absence of any other known pathology however, a reduction in the fibre density remains the most likely interpretation. An optimal acquisition would employ higher b-values, higher angular resolution, and more than one diffusion shell. Future studies using a more suitable acquisition may therefore benefit from the increased statistical power and sensitivity.

5. Conclusion

In this study, we have employed FBA for the first time in depression, demonstrating gender-specific differences in white matter microstructure involving the genu of the corpus callosum (females) and the anterior limb of the internal capsule (males), as well as gender-independent differences in the tapetum that predict remission. We show that FBA reveals a higher volume of abnormalities compared to DTI-based metrics, and that these two techniques identify differing regions which likely reflect different aspects of WM structural differences.

Disclosures

SHK serves as a consultant and has stock options with Brain Resource Ltd.

LMW received non-salary direct research costs as an iSPOT-D investigator from Brain Resource Ltd. She has received fees as a consultant from Psyberguide.

EG is the CEO of Brain Resource Ltd. and has significant equity and stock options in the company.

AJR has received consulting fees from Akili, Brain Resource Inc., Compass Inc., Curbstone Consultant LLC., Emmes Corp, Liva-Nova, Mind Linc., Sunovion, Takeda USA, Taj Medical; speaking fees from Liva-Nova; royalties from Guilford Press and the University of Texas Southwestern Medical Center, Dallas, TX. (for the Inventory of Depressive Symptoms and its derivatives). He is also named co-inventor on two patents: U.S. Patent No. 7,795,033: Methods to Predict the Outcome of Treatment with Antidepressant Medication, Inventors: McMahon FJ, Laje G, Manji H, Rush AJ, Paddock S, Wilson AS and U.S. Patent No. 7,906,283: Methods to Identify Patients at Risk of Developing Adverse Events During Treatment with Antidepressant Medication, Inventors: McMahon FJ, Laje G, Manji H, Rush AJ, Paddock S.

SMG has previously received fees as a consultant for Brain Resource Ltd.

All other authors have no disclosures to declare.

Acknowledgements

SMG acknowledges the support of the Parker-Hughes Bequest and the Heart Research Institute. Brain Resource Ltd. is the sponsor for the iSPOT-D study (NCT00693849). The authors thank Claire Day, BSc, and Catherine King, BSc (global study coordinators) and the iSPOT-D Publication Team. They also acknowledge the hard work of the Brain Dynamics Centre iSPOT-D team at the Sydney site for their help with data collection of the presented cohort. Tim Usherwood, MBBS, PhD, University of Sydney, is thanked for his role in overseeing the partnership with primary care practitioners and recruitment of patients from these primary care settings (as co-principal investigator for the Sydney site). Lavier Gomes, MBBS, and Sheryl Foster, BSc, at the

Department of Radiology at Westmead are thanked for their substantial contributions to MRI data acquisition.

References

American Psychiatric Association, 2000. Diagnostic and Statistical Manual of Mental Disorders, Fourth Edition, Text Revision DSM-IV-TR. American Psychiatric Association.

Andersson, J.L.R., Sotiropoulos, S.N., 2016. An integrated approach to correction for off-resonance effects and subject movement in diffusion MR imaging. NeuroImage 125, 1063–1078.

Andersson, J.L., Skare, S., Ashburner, J., 2003. How to correct susceptibility distortions in spin-echo echo-planar images: application to diffusion tensor imaging. NeuroImage 20, 870–888.

Bergamino, M., Farmer, M., Yeh, H.W., Paul, E., Hamilton, J.P., 2017. Statistical differences in the white matter tracts in subjects with depression by using different skeletonized voxel-wise analysis approaches and DTI fitting procedures. Brain Res. 1669, 131–140.

Bora, E., Fornito, A., Yucel, M., Pantelis, C., 2012. The effects of gender on grey matter abnormalities in major psychoses: a comparative voxelwise meta-analysis of schizophrenia and bipolar disorder. Psychol. Med. 42, 295–307.

Boyd, A., Van de Velde, S., Vilagut, G., de Graaf, R., O'Neill, S., Florescu, S., Alonso, J., Kovess-Masfety, V., Investigators, E.-W., 2015. Gender differences in mental disorders and suicidality in Europe: results from a large cross-sectional population-based study. J. Affect. Disord. 173, 245–254.

Callaghan, F., Maller, J.J., Welton, T., Middione, M.J., Shankaranarayanan, A., Grieve, S.M., 2018. Toward personalized diffusion MRI in psychiatry: improved delineation of fibre bundles with the highest-ever angular resolution in vivo tractography. Transl. Psychiatry 8 (1), 91–99.

Chi, K.F., Korgaonkar, M., Grieve, S.M., 2015. Imaging predictors of remission to antidepressant medications in major depressive disorder. J. Affect. Disord. 186, 134–144.

Drevets, W.C., Price, J.L., Furey, M.L., 2008. Brain structural and functional abnormalities in mood disorders: implications for neurocircuitry models of depression. Brain Struct. Funct. 213, 93–118.

Dyrby, T.B., Lundell, H., Burke, M.W., Reislev, N.L., Paulson, O.B., Ptito, M., Siebner, H.R., 2014. Interpolation of diffusion weighted imaging datasets. NeuroImage 103, 202–213.

Grieve, S.M., Korgaonkar, M.S., Etkin, A., Harris, A., Koslow, S.H., Wisniewski, S., Schatzberg, A.F., Nemeroff, C.B., Gordon, E., et al., 2013a. Brain imaging predictors and the international study to predict optimized treatment for depression: study protocol for a randomized controlled trial. Trials 14, 224.

Grieve, S.M., Korgaonkar, M.S., Koslow, S.H., Gordon, E., Williams, L.M., 2013b. Widespread reductions in gray matter volume in depression. Neuroimage Clin. 3, 332–339.

Hamilton, M., 1960. A rating scale for depression. J. Neurol. Neurosurg. Psychiatry 23, 56–62.

Hua, K., Zhang, J., Wakana, S., Jiang, H., Li, X., Reich, D.S., Calabresi, P.A., Pekar, J.J., van Zijl, P.C., et al., 2008. Tract probability maps in stereotaxic spaces: analyses of white matter anatomy and tract-specific quantification. NeuroImage 39, 336–347.

Jeurissen, B., Leemans, A., Tournier, J.D., Jones, D.K., Sijbers, J., 2013. Investigating the prevalence of complex fiber configurations in white matter tissue with diffusion magnetic resonance imaging. Hum. Brain Mapp. 34, 2747–2766.

Jiang, J., Zhao, Y.J., Hu, X.Y., Du, M.Y., Chen, Z.Q., Wu, M., Li, K.M., Zhu, H.Y., Kumar, P., et al., 2017. Microstructural brain abnormalities in medication-free patients with major depressive disorder: a systematic review and meta-analysis of diffusion tensor imaging. J. Psychiatry Neurosci. 42, 150–163.

Kempton, M.J., Salvador, Z., Munafò, M.R., et al., 2011. Structural neuroimaging studies in major depressive disorder: Meta-analysis and comparison with bipolar disorder. Arch. Gen. Psychiatry 68, 675–690.

Korgaonkar, M.S., Williams, L.M., Song, Y.J., Usherwood, T., Grieve, S.M., 2014. Diffusion tensor imaging predictors of treatment outcomes in major depressive disorder. Br. J. Psychiatry 205, 321–328.

Kuehner, C., 2017. Why is depression more common among women than among men? Lancet Psychiatry 4, 146–158.

Maller, J.J., Broadhouse, K., Rush, A.J., Gordon, E., Koslow, S., Grieve, S.M., 2017. Increased hippocampal tail volume predicts depression status and remission to antidepressant medications in major depression. Mol. Psychiatry 23 (8), 1737–1744.

Maust, D., Cristancho, M., Gray, L., Rushing, S., Tjoa, C., Thase, M.E., 2012. Psychiatric rating scales. Handb. Clin. Neurol. 106, 227–237.

McLean, C.P., Asnaani, A., Litz, B.T., Hofmann, S.G., 2011. Gender differences in anxiety disorders: prevalence, course of illness, comorbidity and burden of illness. J. Psychiatr. Res. 45, 1027–1035.

Mito, R., Raffelt, D., Dhollander, T., Vaughan, D.N., Salvado, O., Brodtmann, A., Rowe, C.C., Villemagne, V.L., Connelly, A., 2017. Fixel-based analysis of fibre tract degeneration in mild cognitive impairment and Alzheimer's disease. Alzheimers Dement. 13, P124–P125.

Mori, S., Crain, B., 2006. MRI Atlas of Human White Matter. Elsevier, Amsterdam.

Pustina, D., Doucet, G., Skidmore, C., Sperling, M., Tracy, J., 2014. Contralateral interictal spikes are related to tapetum damage in left temporal lobe epilepsy. Epilepsia 55, 1406–1414.

Raffelt, D., Tournier, J.D., Rose, S., Ridgway, G.R., Henderson, R., Crozier, S., Salvado, O., Connelly, A., 2012. Apparent Fibre Density: a novel measure for the analysis of diffusion-weighted magnetic resonance images. NeuroImage 59, 3976–3994.

Raffelt, D.A., Smith, R.E., Ridgway, G.R., Tournier, J.D., Vaughan, D.N., Rose, S., Henderson, R., Connelly, A., 2015. Connectivity-based fixel enhancement: Whole-brain statistical analysis of diffusion MRI measures in the presence of crossing fibres. NeuroImage 117, 40–55.

Raffelt, D.A., Tournier, J.D., Smith, R.E., Vaughan, D.N., Jackson, G., Ridgway, G.R., Connelly, A., 2017. Investigating white matter fibre density and morphology using fixel-based analysis. NeuroImage 144, 58–73.

Rigucci, S., Serafini, G., Pompili, M., Kotzalidis, G.D., Tatarelli, R., 2010. Anatomical and functional correlates in major depressive disorder: the contribution of neuroimaging studies. World J. Biol. Psychiatry 11, 165–180.

Sheehan, D.V., Lecrubier, Y., Sheehan, K.H., Amorim, P., Janavs, J., Weiller, E., Hergueta, T., Baker, R., Dunbar, G.C., 1998. The Mini-International Neuropsychiatric Interview (M.I.N.I.): the development and validation of a structured diagnostic psychiatric interview for DSM-IV and ICD-10. J. Clin. Psychiatry 59 (Suppl. 20), 34–57.

Shen, X., Reus, L.M., Cox, S.R., Adams, M.J., Liewald, D.C., Bastin, M.E., Smith, D.J., Deary, I.J., Whalley, H.C., et al., 2017. Subcortical volume and white matter integrity abnormalities in major depressive disorder: findings from UK Biobank imaging data. Sci. Rep. 7, 5547.

Smith, S.M., Nichols, T.E., 2009. Threshold-free cluster enhancement: addressing problems of smoothing, threshold dependence and localisation in cluster inference. NeuroImage 44, 83–98.

Smith, S.M., Jenkinson, M., Johansen-Berg, H., Rueckert, D., Nichols, T.E., Mackay, C.E., Watkins, K.E., Ciccarelli, O., Cader, M.Z., et al., 2006. Tract-based spatial statistics: voxelwise analysis of multi-subject diffusion data. NeuroImage 31, 1487–1505.

Smith, R.E., Tournier, J.D., Calamante, F., Connelly, A., 2013. SIFT: Spherical-deconvolution informed filtering of tractograms. NeuroImage 67, 298–312.

Tournier, J.D., Calamante, F., Gadian, D.G., Connelly, A., 2004. Direct estimation of the fiber orientation density function from diffusion-weighted MRI data using spherical deconvolution. NeuroImage 23, 1176–1185.

Trivedi, M.H., Rush, A.J., Wisniewski, S.R., Nierenberg, A.A., Warden, D., Ritz, L., Norquist, G., Howland, R.H., Lebowitz, B., et al., 2006. Evaluation of outcomes with citalopram for depression using measurement-based care in STAR*D: implications for clinical practice. Am. J. Psychiatry 163, 28–40.

Tustison, N.J., Avants, B.B., Cook, P.A., Zheng, Y., Egan, A., Yushkevich, P.A., Gee, J.C., 2010. N4ITK: improved N3 bias correction. IEEE Trans. Med. Imaging 29, 1310–1320.

Veraart, J., Novikov, D.S., Christiaens, D., Ades-Aron, B., Sijbers, J., Fieremans, E., 2016. Denoising of diffusion MRI using random matrix theory. NeuroImage 142, 394–406.

Vos, T., Allen, C., Arora, M., Barber, R.M., Bhutta, Z.A., Brown, A., Carter, A., Casey, D.C., Charlson, F.J., et al., 2016. Global, regional, and national incidence, prevalence, and years lived with disability for 310 diseases and injuries, 1990–2015: a systematic analysis for the Global Burden of Disease Study 2015. Lancet 388, 1545–1602.

Williams, L.M., Rush, a.J., Koslow, S.H., Wisniewski, S.R., Cooper, N.J., Nemeroff, C.B., Schatzberg, A.F., Gordon, E., 2011. International Study to Predict Optimized Treatment for Depression (iSPOT-D), a randomized clinical trial: rationale and protocol. Trials 12, 4.

Winkler, A.M., Ridgway, G.R., Webster, M.A., Smith, S.M., Nichols, T.E., 2014. Permutation inference for the general linear model. NeuroImage 92, 381–397.

Wright, D.K., Johnston, L.A., Kershaw, J., Ordidge, R., O'Brien, T.J., Shultz, S.R., 2017. Changes in Apparent Fiber Density and Track-Weighted Imaging Metrics in White Matter following Experimental Traumatic Brain Injury. J. Neurotrauma 34, 2109–2118.

Yamada, S., Takahashi, S., Ukai, S., Tsuji, T., Iwatani, J., Tsuda, K., Kita, A., Sakamoto, Y., Yamamoto, M., et al., 2015. Microstructural abnormalities in anterior callosal fibers and their relationship with cognitive function in major depressive disorder and bipolar disorder: a tract-specific analysis study. J. Affect. Disord. 174, 542–548.